Bimodality in macroscopic dynamics of nuclear fission

S.I. Bastrukov, V.S. Salamatin, O.I. Streltsova, I.V. Molodtsova and D.V. Podgainy

Joint Institute for Nuclear Research, 141980 Dubna, Russia

Abstract

The elastodynamic collective model of nuclear fission is outlined whose underlying idea is that the stiff structure of nuclear shells imparts to nucleus properties typical of a small piece of an elastic solid. Emphasis is placed on the macroscopic dynamics of nuclear deformations resulting in fission by two energetically different modes. The low-energy S-mode is the fission due to disruption of elongated quadrupole spheroidal shape. The characteristic feature of the high-energy T-mode of division by means of torsional shear deformations is the compact scission configuration. Analytic and numerical estimates for the macroscopic fission-barrier heights are presented, followed by discussion of fingerprints of the above dynamical bimodality in the available data.

1 Introduction

The underlying assumption of macroscopic treatment of nuclear fission within the framework of liquid drop model (LDM) is that a heavy nucleus can be though of as a small piece of highly incompressible matter governed by equations of hydrodynamics

$$\frac{d\rho}{dt}+\rho\frac{\partial V_i}{\partial x_i}=0 \quad \rho\frac{dV_i}{dt}+\frac{\partial P}{\partial x_i}+\rho_z\frac{\partial U_c}{\partial x_i}=0 \quad \frac{dP}{dt}+\frac{5}{3}P\frac{\partial V_i}{\partial x_i}=0 \quad \Delta U_c=4\pi\rho_z. \tag{1.1}$$

Hereafter ρ is the bulk density, V_i - the velocity, P - the pressure, U_c stands for the Coulomb potential inside sphere uniformly charged with the density ρ_z. The nuclear fission is considered to be dominated by forces of Coulomb repulsion and cohesive surface tension which contribute to the total binding energy of nucleus with comparable amounts [1-3]. One of the basic predictions of LDM is the frequency of electro-capillary vibrations [2]

$$\omega^2=\frac{1}{3}\omega_N^2\,\lambda(\lambda-1)(\lambda+2)\left[1-\frac{20x}{(2\lambda+1)(\lambda+2)}\right]. \tag{1.2}$$

Hereafter by ω_N is denoted the natural unit of frequency and x stands for the parameter of nuclear fissility

$$\omega_N^2=\frac{E_s}{MR^2} \quad x=\frac{E_c}{2E_s} \quad E_s=4\pi\sigma R^2 \quad E_c=\frac{3}{5}\frac{Ze^2}{R}, \quad M=mA \tag{1.3}$$

where $Q=Ze$ and M are the total charge and mass of nucleus, $R=r_0A^{1/3}$ is the nucleus radius, E_s and E_c are the equilibrium surface and Coulomb energies. The instability of quadrupole vibration is regarded as a signature of the commencement of the fission process. The fission-barrier height predicted by LDM reads [4]

$$\mathrm{B_f(LDM)}=\frac{98}{135}E_s^0(1-x)^3. \tag{1.4}$$

It worth noticing that hydrodynamic description implies the absence of any intrinsic ordering of nucleons inside the nucleus. In the meantime, the stiff internal shell structure of single-particle orbitals clearly indicates that the nuclear mean field imparts to nucleus the rigidity typical of a fine peace of an elastic solid. Therefore, it seems to be highly desirable to compare predictions of the elastic globe model (EGM), relayed on the concept of solid like behavior of nuclear matter with those inferred from the liquid drop model based on the assumption that continuous nuclear matter is governed by equations of hydrodynamics (1.1).

2 Elastodynamic treatment of nuclear collective dynamics

Studying of the nuclear collective dynamics on the basis of model of an elastic sphere has been initiated in Ref.[5] after the discovery of giant multipole resonances with $\lambda \geq 2$. Modelling a heavy nucleus by a small particle of an elastic Fermi-continuum it has been found, that the collective dynamics of nucleons accompanying the giant-resonance response can be adequately described in terms of eigevibrations of an elastic sphere. This approach rests on the statement that the motions of macroscopic nuclear matter subject to the equations of elastodynamics.

$$\frac{d\rho}{dt} + \rho\frac{\partial V_i}{\partial x_i} = 0 \tag{2.1}$$

$$\rho\frac{dV_i}{dt} + \frac{\partial P_{ik}}{\partial x_k} + \rho\frac{\partial U_c}{\partial x_i} = 0 \qquad \Delta U_c = 4\pi\rho_z \tag{2.2}$$

$$\frac{dP_{ij}}{dt} + P_{ik}\frac{\partial V_j}{\partial x_k} + P_{jk}\frac{\partial V_i}{\partial x_k} + P_{ij}\frac{\partial V_k}{\partial x_k} = 0. \tag{2.3}$$

Based on these equations the nuclear vibrations have been studied in Refs.[6, 7] with the restoring force dominated by quadrupole deformations of the nuclear Fermi-surface (originating from coherent distortions of shells without spoiling the initial ordering of single particle orbitals).

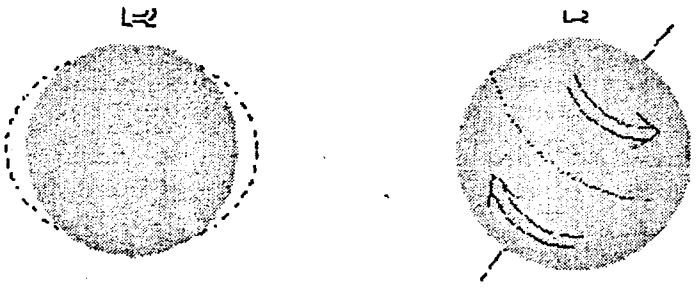

Figure 1: Geometrical picture of spheroidal and torsional quadrupole vibrations

It has been found the giant electric ($E\lambda$) and the giant magnetic ($M\lambda$) modes can be interpreted as manifestation of spheroidal and torsional vibrations (see Fig.1) of a heavy nucleus modelled by a spherical mass of an elastic Fermi-solid. Analytic estimates for the energy of

the nuclear giant electric [6] and giant magnetic [7-9] resonances with $\lambda \geq 2$ computed in the elastodynamic nuclear model are given by

$$E(E\lambda) = \hbar\omega_F \left[\frac{2}{5}(2\lambda+1)(\lambda-1)\right]^{1/2} \qquad E(M\lambda) = \hbar\omega_F \left[\frac{1}{5}(2\lambda+3)(\lambda-1)\right]^{1/2} \tag{2.4}$$

where $\omega = v_F/R$ is the natural unit of resonant frequency, v_F is the Fermi-velocity (radius of the Fermi-sphere in the momentum space) and R is the nucleus radius. The resultant general trends for the energy, spread width and total excitation strength are found to be in fairly reasonable agreement with data throughout the periodic table (see for instance [8] and references therein).

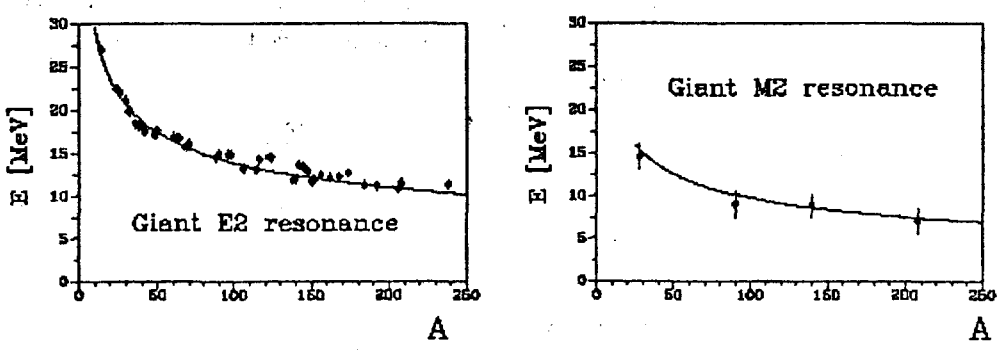

Figure 2: Energy vs mass number of the giant quadrupole electric and magnetic resonances computed on the basis of elastodynamic nuclear model, eqs.(2.4).

With this in mind, one can expect that the elasticity of nuclear matter revealed in the resonance nuclear response should be traced in the macroscopic dynamics of nuclear fission, too. Guided by this motivation, in Refs. [10-14] the elastodynamic model of nuclear fission has been developed as a counterpart of liquid drop model. Here we report some latest calculation of macroscopic barriers of nuclear fission accentuating the dynamical bimodality of the fission process coming from the model.

3 Nuclear fission in the elastic globe model

In the elastic globe model a heavy nucleus is thought of as a small uniformly charged particle of an elastic solid governed by equations of elastodynamics (2.1)-(2.3). Taking into account that the fission process is dominated by cohesive surface and disruptive electric forces, in Ref.[12], Hamiltonian of electro-elastic vibrations

$$H = \frac{M\alpha^2}{2} + \frac{K\alpha^2}{2}, \qquad \omega^2 = \frac{K}{M}, \tag{3.5}$$

$$M = \int \rho_0 a_i\, a_i\, dV, \quad K = \oint \left[P_s \left(\frac{\partial a_i}{\partial x_j} + \frac{\partial a_j}{\partial x_i} \right) a_j \right] dS_i - \frac{1}{2} \int P_c \left(\frac{\partial a_i}{\partial x_j} + \frac{\partial a_j}{\partial x_i} \right)^2 dV$$

$$P_c(\mathrm{r}) = -\frac{2\pi}{3} \rho_z^2 (r^2 - R^2) \qquad P_s = \frac{2\sigma}{R} \tag{3.6}$$

has been derived. The elastic displacements a are found as the solutions to the vector Laplace's equation: $\Delta\, \mathbf{a}(\mathrm{r}) = 0$, $\mathrm{div}\, \mathbf{a}(\mathrm{r}) = 0$: the poloidal $\mathbf{a}_p$ corresponding to spheroidal vibrations and the toroidal field $\mathbf{a}_t$ describing torsional vibrations

$$\mathbf{a}_p = \frac{N_p}{\lambda + 1} \,\mathrm{rot}\,\mathrm{rot}\,\mathrm{r}\, r^\lambda\, P_\lambda(\mu)\, \alpha(t) = N_p\, \mathrm{grad}\, r^\lambda\, P_\lambda(\mu), \quad \mathbf{a}_t = N_t\, \mathrm{rot}\,\mathrm{r}\, r^\lambda\, P_\lambda(\mu). \tag{3.7}$$

Hereafter $P_\lambda(\mu)$ is the Legendre polynomial of the multipole order λ and $\mu = \cos\theta$. The frequency of spheroidal and torsional electro-elastic modes computed within the EGM [12,13] are given by

$$\omega_s^2 = \frac{4}{3}\omega_N^2 (2\lambda + 1)(\lambda - 1) \left[1 - \frac{5x}{(2\lambda + 1)} \right] \quad \omega_t^2 = \frac{2}{3}\omega_N^2 (2\lambda + 3)(\lambda - 1) \left[1 - \frac{5x}{(2\lambda + 3)} \right].$$

It is remarkable that in contrast to LDM, the EGM permits two kind of collective motions resulting in fission. Regarding the low-energy S-mode, EGM leads to the conclusions very similar to those inferred in LDM. In particular, both EGM and LDM predict onset of instability of quadrupole spheroidal vibration when $x = 1$. The capability of supporting torsional vibrations accompanied by magnetic γ-radiation is the major feature distinguishing nuclear oscillatory dynamics in the elastic globe model from that in the liquid drop model [9]. The instability of nucleus with respect to torsional electro-elastic quadrupole deformation resulting from the condition $\omega_t(\lambda = 2) = 0$ is characterized by $x = 7/5$. The macroscopic energy of elastic deformation is given by

$$E = \int_v \frac{\partial \sigma_{ij}}{\partial x_j} \xi_i\, dv = \int_s \sigma_{ij} \xi_i\, ds_j - \int_V \sigma_{ij} \frac{\partial \xi_i}{\partial x_j}\, dv \quad \sigma_{ij} = P\, u_{ij} \quad u_{ij} = \frac{1}{2} \left(\frac{\partial \xi_i}{\partial x_j} + \frac{\partial \xi_j}{\partial x_i} \right).$$

The latter equation can be represented as a sum of the surface E_s and the Coulomb E_c energies

$$E = E_s + E_c. \quad E_s = P_s \int_S u_{ij}\, \xi_i\, dS_j = P_s \int_V u_{ij}\, u_{ij}\, dV \quad E_c = -\int_V P_c u_{ij}\, u_{ij}\, dV. \tag{3.8}$$

Both spheroidal and torsional deformations are computed on equal footings.

3.1 Spheroidal mode of fission

We confine our analysis to spheroidal deformations of the form $R(\alpha_2, \alpha_3) = R[1 + \alpha_2 P_2(\mu) + \alpha_3 P_3(\mu)]$. For the poloidal displacements

$$\boldsymbol{\xi}(\mathrm{r}, \alpha) = \mathbf{a}_p^\lambda(\mathrm{r})\, \alpha_\lambda \quad \mathbf{a}_p^\lambda = \frac{N_p^\lambda}{\lambda + 1} \,\mathrm{rot}\,\mathrm{rot}\,\mathrm{r}\, r^\lambda\, P_\lambda(\mu) \quad N_p^\lambda = \frac{3}{\lambda(2\lambda + 1) R^{\lambda - 2}} \tag{3.9}$$

calculation of the energy of elastic deformation yields

$$E = \frac{9}{25}E_s\left[(1-x)\alpha_2^2+\frac{1}{5}(3-10x)\alpha_2^4\right]+\frac{12}{49}\left[\left(1-\frac{5}{7}x\right)\alpha_3^2+\frac{13}{25}\left(1-\frac{50}{21}x\right)\alpha_3^4\right]$$
$$+ \frac{144}{1225}(1-x)\alpha_2\alpha_3^2+\frac{2871}{8575}\left(1-\frac{18890}{6699}x\right)\alpha_2^2\alpha_3^2. \qquad (3.10)$$

This function is pictured in Fig.3 for U^{234} with the set of parameters borrowed from [19] (see also [13]).

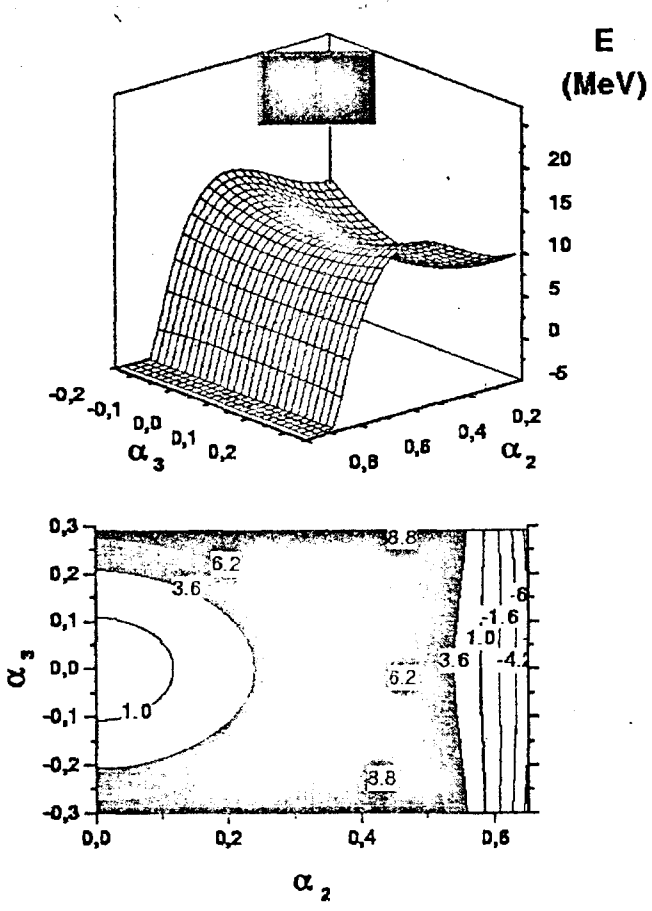

Figure 3: The fission valley and its landscape for two heavy nuclei in accordance with predictions of equation (3.10).

For quadrupole deformation $R(\alpha_2) = R[1 + \alpha_2 P_2(\mu)]$, the above equation for the energy of elastic spheroidal deformations is replaced by [13]

$$E(\alpha_2) = \frac{9}{25} E_s \left[(1-x)\alpha_2^2 + \frac{1}{5}(3-10x)\alpha_2^4 \right]. \tag{3.11}$$

The fission-barrier height for the S-mode is given by

$$\mathrm{B_{sf}(EGM)} = \frac{9}{20} E_s \frac{(1-x)^2}{(10x-3)}. \tag{3.12}$$

In Fig.4, theoretical predictions of (3.12) are compared with data taken from [16, 17, 18].

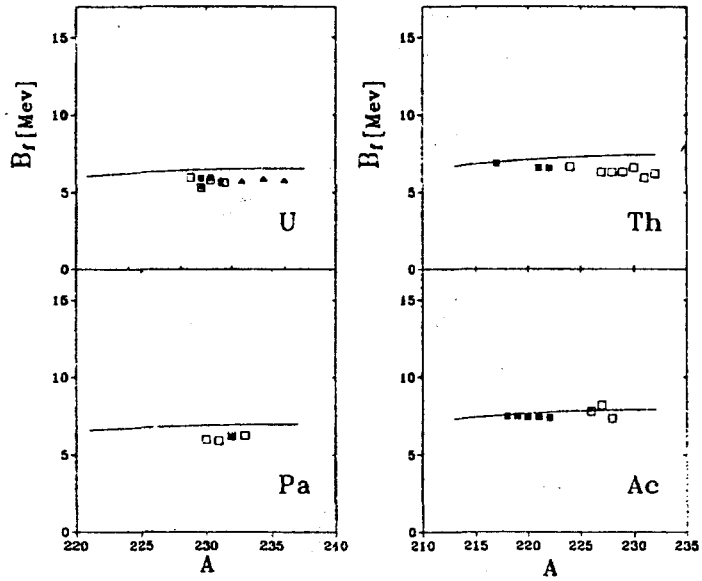

Figure 4: Comparison of EGM computed barriers (lines) with data.

The basic conclusion is that the elastic globe model recovers all the prediction of the liquid drop model regarding the macroscopic characteristics of nuclear fission by means of disruption of quadrupole spheroidal configuration.

3.2 Torsional mode of fission

To get a feeling about fission in torsional channel we consider a highly ideilized deformation, pictured in Fig.5., given by equation

$$R = R_0 \left[1 + \phi_2 \frac{dP_2(\mu)}{d\mu} \right]. \tag{3.13}$$

The energy of quadrupole torsional deformation computed with the toroidal field of shear displacements

$$\xi(\mathbf{r}, \phi) = \mathbf{a}_t^\lambda(\mathbf{r})\, \phi_\lambda \quad \mathbf{a}_t^\lambda = N_t^\lambda \,\mathrm{rot}\, \mathbf{r}\, r^\lambda P_\lambda(\mu) \quad N_t^\lambda = \frac{1}{R^{\lambda-1}} \tag{3.14}$$

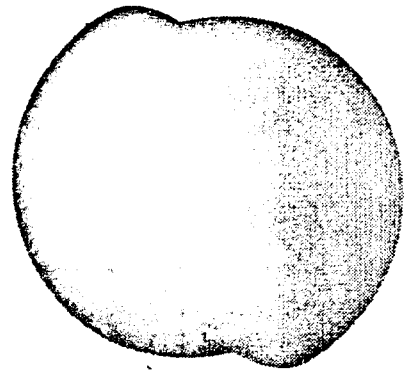

Figure 5: Schematic illustration of the scission configuration in the torsional mode of fission.

is given by

$$E(\phi_2) = \frac{6}{5}E_s^0\left[(1-\frac{5}{7}x)\phi_2^2 + \frac{9}{5}(21-50x)\phi_2^4\right]. \tag{3.15}$$

For the fission-barrier height we obtain

$$\mathrm{B_{tf}} = \frac{1}{42}E_s^0\frac{(7-5x)^2}{(50x-21)}. \tag{3.16}$$

Comparison of the EGM computed fission-barrier heights with macroscopic experimental barriers is presented in Fig.6.

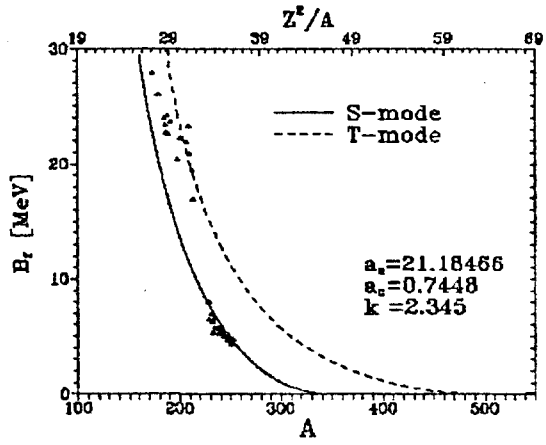

Figure 6: EGM computed macroscopic fission-barrier heights (curves) and experimental macroscopic barriers (symbols).

4 Summary

Thus, the EGM predicts dynamical bimodality of nuclear fission in two energetically different channels. The fission-barrier height for T-mode is higher than for S-mode. Since the torsional mode is characterized by compact scission shape (Fig.5), one can expect that the total kinetic energy of outgoing fragments must be higher as compared to that for s-mode. The signatures of such a behavior of TKE have been disclosed in experiments on fission of uranium isotopes by fast neutrons, reported in [20]. From comparison general trends in data and theoretical predictions of the EGM plotted in Fig.6 one can conclude that the macroscopic dynamics of fission of the middle weight nuclei (with mass numbers $170 < A < 210$) is dominated by torsional mechanism of disintegration whereas the low-energy fission of the heavy and superheavy elements is governed by spheroidal deformation.

References

[1] Greiner W. & Maruhn J.A. *Nuclear Models* (Springer, Berlin, 1996).

[2] Wilets L. *Theories of Nuclear Fission* (Clarendon, Oxford, 1964).

[3] Vandenbosch R. & Huizenga J.R. *Nuclear Fission* (Academic, New York, 1973).

[4] Bohr A & Mottelson B., *Nuclear Structure* (World Scientific, Singapore, 1998) Vol.2.

[5] Bertsch G.F., Ann. Phys. Rev. **86** (1974) 138.

[6] Nix J.R. & Sierk A.J., Phys. Rev. **C21** (1980) 396.

[7] Bastrukov S. & Gudkov V., Z. Phys. **A341** (1992) 395.

[8] Bastrukov S. & Molodtsova I., Phys. Part. Nucl. **26** (1995) 180.

[9] Bastrukov S. Libert J. & Molodtsova I., Int. J. Mod. Phys. **E6** (1997) 89.

[10] Bastrukov S., Molodtsova I. & Yuldashbaeva E.: *Phys. Atom. Nucl.* **57** (1994) 1177.

[11] Bastrukov S. & Molodtsova I.: *Physics-Doklady* **41** (1996) 388.

[12] Bastrukov S. & Podgainy D., Physica **A250** (1998) 435.

[13] Bastrukov S., Podgainy D., Molodtsova I. & Kosenko G., J. Phys. **G24** (1998) L1.

[14] Bastrukov S., Podgainy D., Molodtsova I., Kosenko G. & Salamatin V., in *Heavy Ion Collisions* (World Scientific, Singapore 1998) Eds. Yu. Oganessian and R. Kalpakchieva.p.640.

[15] Möller P., Nix J.R., Myers W.D. & Swiatecki W.J., *At. Data Nucl. Tables* **59** (1995) 185.

[16] Dalhlinger M., Vermeulen V. & Schmidt K.H., *Nucl. Phys.* **A376** (1982) 93; Grewe A. et al., *Nucl. Phys.* **A614** (1997) 400.

[17] Myers, W. D. & Swiatecki, W. J., Nucl. Phys. **A612** (1997) 249.

[18] Sierk A.J., *Phys. Rev.* **C33** (1986) 2039; Mashnik S.G., *Acta Phys. Slovaca* **43** (1993) 243.

[19] Möller P., Nix J.R., Myers W.D. & Swiatecki W.J., *At. Data Nucl. Tables* **59** (1995) 185.

[20] Goverdovski A.A. & Mitrofanov V.F., in *Heavy Ion Collisions* (World Scientific, Singapore 1998) Eds. Yu. Oganessian and R. Kalpakchieva. p. 699.